3D radiative transfer under conditions of non local thermodynamic equilibrium: A contribution to the numerical solution

Doris Folini[1,2] and Rolf Walder[1,3]

Abstract. A new approach to the solution of the 3D NLTE optically thick radiative transfer problem for moving media is presented. The radiative transfer problem basically consists of determining consistent values for the radiation field and the state of the matter. A first task, therefore, is the solution of the radiative transfer equation, which describes the propagation of radiation in the presence of matter. The second task is the determination of the state of the matter in the presence of a radiation field. These two parts are then coupled iteratively. We present the first application of the generalized mean intensity approach, suggested by Turek [9], [10] for the solution of the radiative transfer equation, to NLTE problems. The resulting linear system is solved using BiCGStab. The corresponding code has successfully been applied to some first test problems.

1. Introduction

The problem of radiative transfer is crucial in astrophysics. Most information we have from objects in the universe reaches us in the form of radiation and the physics of many astrophysical objects is essentially influenced by strong radiation fields. For example, radiation fields play a significant role in the driving of most stellar winds. They are important for the energy transport in accretion disks and young stellar objects, and it has been suggested that they contribute to the complex shaping of planetary nebulae. The radiation we observe with our telescopes contains information about the physical conditions where it emerged as well as about the conditions on the way to us. To retrieve this information from an observed spectrum usually requires model simulations, in particular when, which is the rule, the distant object being observed appears as a point source only. It is this kind of astrophysical problems which to attack is our task. The complexity of the problem, however, also requires us to make use of the best numerical techniques we can access.

The problem of radiative transfer under conditions of non-local thermodynamic equilibrium (NLTE) basically consists of determining consistent values for the radiation field and the state of the matter. In the frame of this work, the state of the matter includes the ionization state of the matter and the atomic level

populations, while the dynamics of the matter is assumed to be known. The problem can then be regarded as being divided into two parts: the radiative transfer equation, which describes the transport of radiation in the presence of matter, and the statistical equilibrium equations together with some conservation laws, which describe the state of the matter in the presence of a radiation field.

Our approach follows this partition. This means that, first, a solver for the radiative transfer equation is required, second, a solver for the statistical equilibrium part is needed, and, third, these two parts have to be coupled in a favorable way. Each of these three parts has its own difficulties. In addition, the storage requirements are enormous, at least for multi dimensions, as at each spatial grid point the radiation field for each frequency and the populations of all atomic levels and ionization stages have to be stored. While for one dimensional problems well established methods exist in the astrophysical community (see e.g. Hubeny [4]) the solution of the multidimensional problem is still in its infancy. Among the most recent multidimensional approaches to the problem are those of Fabiani Bendicho, Trujillo Bueno, and Auer [2], of Dykema, Klein, and Castor [1], of Stone, Mihalas, and Norman [8], and, for the transfer equation alone, of Kanschat [5] and Turek [9], [10]. The present approach takes up the idea of Turek for the solution of the radiative transfer equation. He suggested to solve for a generalized mean intensity instead of directed intensities. Although the entire radiative transfer problem is solved, including the statistical equilibrium equations, the strength of the present approach lies in the solution of the transfer equation itself.

Although the approach presented here aims at radiative transfer for astrophysical applications it seems worth mentioning the wide variety of other applications. The general problem of radiative transfer occurs in such different fields as room climate engineering, temperature measurements of melts, the optimization of combustion devices, atmospherical sciences, or in connection with laser technology.

The organization of this paper is as follows. In section 2 the solution of the radiative transfer equation is outlined and the convergence properties of BiCGStab, applied to the discretized transfer equation, are analyzed. Section 3 deals with the statistical equilibrium equations and section 4 adresses the question of parallelization. Finally, section 5 is devoted to discussion and conclusions.

2. Solution of the transfer equation

The transfer equation to be considered describes non-relativistic, stationary, frequency decoupled, and unpolarized radiative transfer. For a particular direction of propagation $n \in S^2$ it is given by

$$\begin{aligned} n\nabla_x I(x,n,\nu) + \chi(x,n,\nu) I(x,n,\nu) = \\ \lambda(x,\nu) \int_{S^2} P(n,n') I(x,n',\nu) d\omega' + f(x,n,\nu) \\ \text{in} \qquad D_1 \times S^2 \times D_2. \end{aligned} \tag{1}$$

Here $I(x, n, \nu)$ denotes the specific or directed intensity at point $x \in D_1$ and frequency $\nu \in D_2$ propagating in direction $n \in S^2$. It has to be emphasized that the integral term couples all directions $n \in S^2$ and that, therefore, such a transfer equation has to be solved for each direction $n \in S^2$. The coefficient f stands for atomic emission, λ is the scattering coefficient, and $\chi = \kappa + \lambda$ describes the total losses. κ is the absorption coefficient and $P(n, n')$ is the scattering redistribution function. It should be stressed that χ, λ, and f depend on the atomic level populations which, in turn, depend on the radiation field described by $I(x, n, \nu)$. The computation of these level populations and the coupling to the transfer equation are outlined in section 3. Further, $D_1 \subset R^3$, S^2 is the unit sphere in R^3, $D_2 \subset R^1$, n is the unit vector in the direction of propagation of I, $d\omega$ is the solid angle element associated with n. The boundary conditions are problem dependent and will not be considered here any further.

2.1. Discretization

FREQUENCY DISCRETIZATION: The transfer equation as given in equation 1 is decoupled in frequency. The choice of discrete frequency points is guided by the physics, for example by the location of ionization edges and spectral lines. Due to the decoupling of the transfer equation with respect to frequency, the frequency indices will be omitted in the following. One should bear in mind, however, that I, χ, λ, and f actually depend on frequency.

DISCRETIZATION OF S^2: A parameterization of S^2 over $[0, 2\pi] \times [0, \pi]$ is used, choosing the discrete ordinates n^m equidistantly in both intervals. For these directions $I(n^m)$ is computed. Using the same directions the trapezoidal rule is used for the integral over the sphere, with $K + 1$ support points on $[0, \pi]$ and $L + 1$ points on $[0, 2\pi]$:

$$\int_{S^2} P(n, n') I(n') d\omega' \approx \sum_{k=1}^{K-1} \sum_{l=0}^{L-1} c^{lk}(P) I(\phi^l, \theta^k) = \sum_{m=1}^{M} c^m(P) I^m, \qquad (2)$$

where $M \equiv (K - 1)L$. For the special choice of $P(n, n') = 1/4\pi$ the quadrature weights become $c^{lk} = \frac{\pi}{2KL} sin\theta^k$.

The resulting, physically unnecessary, concentration of discrete ordinate directions near the poles of the sphere at $\theta = 0$ and $\theta = \pi$ can be partly overcome by omitting some of the ordinates in ϕ-direction towards the poles, such that $\Delta\phi$ at latitude θ is at least $1/2\Delta\phi_{equator}$, a procedure which is physically well justified.

Using the discrete ordinate directions n^m defined above and writing I^m instead of $I(n^m)$ the transfer equation discretized over S^2 and for a particular direction n^m, $m \in \{1, ..., M\}$, becomes

$$n^m \nabla_x I^m(x) + \chi^m(x) I^m(x) = \lambda(x) \sum_{m=1}^{M} c^m(P) I^m(x) + f^m(x). \qquad (3)$$

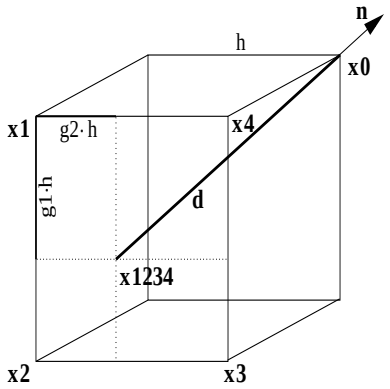

FIGURE 1. Spatial discretization of the transport term in 3D.

SPATIAL DISCRETIZATION: For the spatial discretization a Cartesian grid is used. The transport part is discretized using a first order finite difference scheme together with upwinding. Figure 1 illustrates the discretization of the transport term at point x_0 in 3D. Denoting by I^m_* the discrete approximation to I^m at point x_*, where $* = \{0,1,2,3,4\}$, the discretization of the transport term is given by

$$\begin{aligned} n^m \nabla_x I^m(x_0) &= \frac{I^m_0 - I^m_{1234}}{d} + O(h) \\ &= d^{-1}\left[I^m_0 - I^m_1\left(1 - g_1 - g_2 + g_1 g_2\right) - \right. \\ &\quad \left. I^m_2\left(g_1 - g_1 g_2\right) - I^m_3\left(g_1 g_2\right) - I^m_4\left(g_2 - g_1 g_2\right)\right] + O(h) \end{aligned} \quad (4)$$

Now let I^m_h denote the vector containing the specific intensity of direction n^m at each discrete grid point. The transfer equation for one frequency point can then be written as

$$T^m_h I^m_h = L_h \sum_{m=1}^{M} c^m(P) I^m_h + f^m_h. \quad (5)$$

Here T^m_h describes the discretized transport term as well as the discretized loss coefficient $\chi^m(x_0)$. L_h and f^m_h stand for the discretized scattering and emission coefficients at point x_0 on the right hand side of equation 3. It should be noted that this spatial discretization gives good results only for χh considerably smaller than 1. This may be illustrated by the special case of a transfer equation of the form $\partial I/\partial x + \chi I = 0$, with $\chi = const.$, whose analytical solution is given by $I_2 = I_1 \cdot e^{-h\chi}$ with $h = x_2 - x_1$, while the above discretization yields $I_2 = I_1/(1+\chi h)$.

2.2. The generalized mean intensity approach

The generalized mean intensity is given by

$$\tilde{J}(x) = \int_{S^2} P(n,n') I(x,n') d\omega' \quad (6)$$

or, in its discrete version, by

$$\tilde{J}_h = \sum_{m=1}^{M} c^m(P) I_h^m, \tag{7}$$

where now $\tilde{J}_h$ denotes the vector containing the discrete generalized mean intensities at each spatial grid point. Remembering that $P(n,n')$ can depend on angle, it can be seen that $\tilde{J}_h$ deviates from the physical mean intensity

$$J(x) = \frac{1}{4\pi} \int_{S^2} I(x,n') d\omega' \tag{8}$$

by the term $P(n,n')$ in the integral if $P(n,n') \neq 1/4\pi$.

Equation 5 can now be rewritten in terms of the discretized generalized mean intensity $\tilde{J}_h$. For this purpose the quadrature sum in the equation is replaced by $\tilde{J}_h$ and the operator T_h^m is inverted and taken to the right hand side. Applying now a quadrature sum over all ordinate directions to the entire equation over all ordinate directions, using again the function $P(n,n')$, leads to

$$\begin{aligned} \tilde{J}_h &= \sum_{m=1}^{M} c^m(P) \left(T_h^m\right)^{-1} L_h \tilde{J}_h + \sum_{m=1}^{M} c^m(P) \left(T_h^m\right)^{-1} f_h^m \\ &= T_h L_h \tilde{J}_h + F_h. \end{aligned}$$

Taking all $\tilde{J}_h$ terms to the left one obtains

$$A_h \tilde{J}_h = F_h. \tag{9}$$

where $A_h = 1 - T_h L_h$. For the special choice of $P(n,n') = 1/4\pi$ this is an equation for the discrete counterpart of the physical mean intensity. If desired, the specific intensities I_h^m can be recovered from $\tilde{J}_h$ by solving equation 5 with the quadrature sum replaced by $\tilde{J}_h$.

Note that it is possible to invert T_h^m efficiently if it is brought to lower triangular form. This can be achieved due to the upwinding requirement and by an appropriate renumbering of the grid points, depending on the ordinate direction.

2.3. Iterative solution: analysis of the convergence behavior

For the solution of equation 9, the BiCGStab algorithm developed by Van der Voerst [11] is used. Its advantages are that it is applicable to non-symmetric problems as the one presented here, that its memory requirements are rather small, and that it usually shows a rather smooth and fast convergence. As it works reasonably well for the problems considered up to now no other solver has been tested. A solution is assumed to have converged if the l_2-norm of the BiCGStab residual is smaller than a prescribed tolerance ϵ.

In the following, the convergence properties of the diagonally preconditioning BiCGStab are analyzed. (See also the note below on preconditioning). Here only the numerical results are presented. An analytical analysis leading to the same qualitative results can be found in Folini [3].

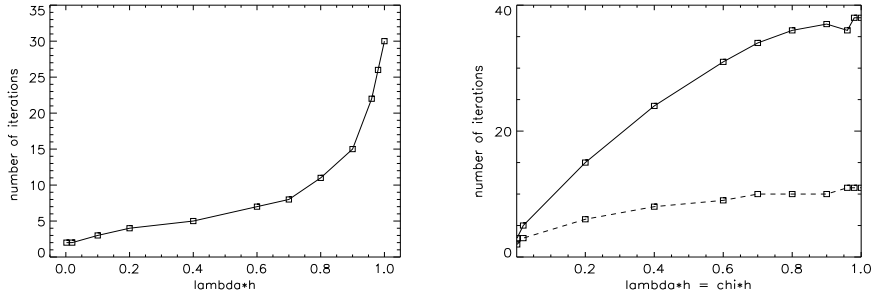

FIGURE 2. **Left:** Convergence of BiCGStab as a function of λh for fixed $\chi = 50$, $h = 0.02$, for test example 2. **Right:** Convergence of BiCGStab as a function of $\lambda h = \chi h$ for test example 1 and two different grid spacings. The solid line denotes $h = 0.02$, the dashed line $h = 0.1$. Note that the different convergence behaviour is not due to h but to χ. For details see text.

Test example 1: The computational domain is given by $[0,1]^3$. A square shaped beam is considered, entering the computational domain at the boundary $x = 0$. It is directed along the discrete ordinate direction ($\phi = 0, \theta = \pi/2$) which is parallel to the positive x-direction. Its axis goes through the point $(x, y, z) = (0, 0.5, 0.5)$ and it has a cross-section of 0.41×0.41. The specific intensity I of the beam is set to 10^4 at the incoming boundary. $(n_\phi, n_\theta) = (24, 13)$ ordinates have been used. The error bound for BiCGStab was set to $\epsilon = 10^{-10}$. χ, λ, and h are variable and given along with the individual test cases.

Test example 2: The same as test example 1, but using $(n_\phi, n_\theta) = (16, 7)$ ordinates.

Convergence as a function of λ for $\lambda h \to \chi h$: Figure 2 (left) shows the convergence behavior of preconditioned BiCGStab as a function of λh for fixed $\chi = 50$ and $h = 0.02$ with $\chi h = 1$. The convergence properties depend strongly on the value of λh and start to deteriorate strongly above $\lambda h \approx 0.7$. In physical terms this means that the convergence properties are quite good as long as scattering contributes less than about 70% to the total losses.

Convergence as a function of $\chi h = \lambda h$: Considering the 'worst case' (see figure 2, left) $\chi h = \lambda h$, for increasing χh figure 2 (right) illustrates that the number of iterations increases quite rapidly already for relatively small values of $\chi h = \lambda h$. Physically speaking, this means that the convergence properties deteriorate already for a small extinction term χ if this extinction is mostly due to scattering.

Convergence as a function of h: Figure 3 (left) shows that the convergence properties hardly depend on the grid spacing h, at least for the above test example and for the 'worst case' $\chi = \lambda$. While h is reduced by a factor of 5, from $h = 0.1$ to $h = 0.02$, the number of iterations increases at most by 36%. For a more detailed discussion of this h dependence see Folini [3].

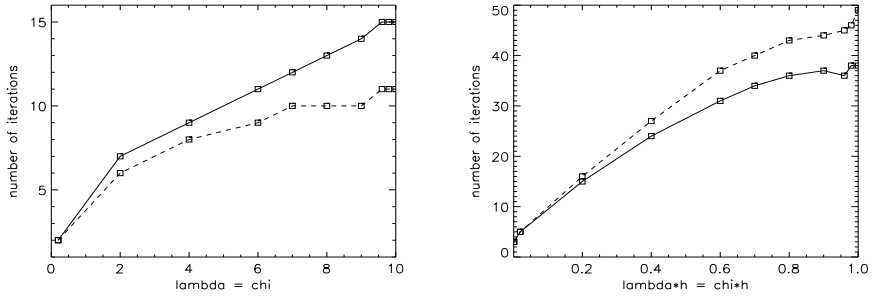

FIGURE 3. **Left:** Convergence behaviour of BiCGStab as a function of $\lambda = \chi$ for test example 1 and two different grid spacings. The solid line denotes $h = 0.02$, the dashed line $h = 0.1$. **Right:** Convergence behaviour of preconditioned (solid line) and unpreconditioned (dashed line) BiCGStab as a function of $\chi h = \lambda h$ with $h = 0.02$ for test example 1.

Convergence for non-constant χ and λ: One additional test was performed with test example 1 for the following, non-constant, choice of χ and λ: $\chi = \lambda = 5$ for $x < 0.5$ and $\chi = \lambda = 50$ for $x \geq 0.5$. In this case 26 iterations were needed. For comparison, the same example but with $\chi = \lambda = 5$ in the entire domain requires 10 iterations, for $\chi = \lambda = 50$ in the entire domain 38 iteration are needed.

Conclusions: The convergence properties of BiCGStab are strongly determined by the ratio λ/χ. If for constant χ and λ the ratio λ/χ increases convergence will slow down, even for relatively small values of χh. For small ratios the convergence will be fast, even for $\chi h = 1$. If the ratio varies over the computational domain the convergence will be better than for the maximum ratio alone and the number of iterations will lie somewhere between the number of iterations required for the maximum and minimum ratio alone. If $\lambda \approx \chi$ the number of iterations increases with increasing χ for constant χh. The grid spacing h has hardly any influence on the number of iterations.

A note on preconditioning: Preconditioning here is difficult for several reasons. As A is a full matrix it cannot be stored and it is necessary to implement the problem in a matrix free way. A itself is never computed explicitly. This makes it difficult to analyze A and to extract parts of A for use as a preconditioner. Also, many entries are of roughly the same size and A is neither necessarily diagonally dominant nor is it symmetric. As already mentioned, in a first attempt, diagonal preconditioning is used and BiCGStab is applied to the preconditioned system $D^{-1}AJ = D^{-1}F$ where $D = diag\{A\}$. However, figure 3 (right) indicates that, at least for the considered example, this hardly reduces the number of iterations and that the overall computational costs may even increase. But under the above mentioned conditions, the search for a good preconditioner is a demanding task.

3. Statistical equilibrium equations and coupling

The coefficients χ, λ, and f of the radiative transfer equation at each spatial grid point are determined by the atomic level populations N_r at the corresponding grid point. The second big task in optically thick NLTE radiative transfer, therefore, is the determination of these atomic level populations N_r at each spatial grid point. The populations are determined by a non-linear system of equations, consisting of several conservation laws and the actual statistical equilibrium equations for the individual level populations,

$$\frac{dN_r}{dt} = \sum_{s \neq r} (R_{sr} + C_{sr}) N_s - (R_{rs} + C_{rs}) N_r. \tag{10}$$

The transition probabilities R_{sr} depend on the radiation field, the probabilities C_{sr} depend on the electron density. Both R_{sr} and C_{sr} depend on the temperature of the matter, which in turn is a function of N_r and the radiation field.

In general, the solution of this non-linear system can be rather delicate. First, the resulting population numbers easily differ by more than ten orders of magnitude. Second, the non-linearities not only require an iterative solution but, possibly more important, may allow for more than one stationary solution. For example, bistable solution exist if molecules are considered (see e.g. Bourlot et al. [6]).

In the present approach only stationary situations are considered. The appropriate electron density N_e to fulfill charge conservation is determined by fix-point iteration, computing N_e for given N_r, then computing new coefficients C_{sr} for the statistical equilibrium equations, and so on. The remaining linear system of algebraic equations presently consists of some ten equations, which is small enough to be solved by Householder transformations. It should be noted here that in 1D problems often several thousand equations are considered instead. These systems then require other solution techniques than just Householder transformations. Optically thick lines are treated in the frame of slightly extended Sobolev theory. Details on this point can be found in Folini [3].

Having solvers for the transfer equation and the statistical equilibrium equation part the two now have to be brought together. In the frame of this work only pure fix-point iteration between the two parts is applied. The simulation is assumed to have converged if between succeeding iterations the relative changes of all level populations and of the radiation field are smaller than a given global tolerance. However, from 1D simulations it is known that under extreme conditions (very high matter density, for example) mere iteration between the transfer equation and the rate equation part often fails. Several approaches have been suggested to overcome this problem. Among them are the so called ALI, MALI, and MUGA techniques (see e.g. Hubeny [4], Rybicki and Hummer [7], Fabiani Bendicho [2]), where the basic idea is to incorporate part of the transfer operator into the statistical equilibrium equations.

4. Aspects of parallelization

Due to the huge memory and CPU requirements multidimensional NLTE radiative transfer is a candidate for parallelization, preferably on distributed memory machines. Up to now we have parallelized the transfer part using MPI. In fact, the radiative transfer problem as considered here is very well suited for parallelization. Being decoupled in frequency, the transfer part can be split according to frequency. The rate equation part can be treated by domain decomposition. Load balancing, however, is difficult in real size problems. The coefficients of the transfer equation depend strongly on frequency and so does the number of iterations which can be hardly estimated a priori. The convergence properties of the rate equations can also vary considerably from point to point making an a priori estimate of the work to be done again difficult. Also the practical implementation on distributed memory machines is somewhat delicate. For the present problem the distribution of the memory among different nodes requires that most of the memory has to be communicated twice in each global iteration step, because the solution of the transfer equation for one particular frequency point needs data for this frequency point for all the spatial grid points, while the solution of the rate equation part at one particular spatial grid point needs data for this grid point and for all frequencies. Although the time required for this communication is not too important, as one global iteration step takes much longer anyhow, the 'logistics' of the memory exchange are quite difficult to program. From this point of view shared memory machines seem better suited, but they usually offer less memory.

5. Discussion and conclusions

The numerical solution of the multidimensional, NLTE radiative transfer problem is still in its infancy. Only very few groups have attack this problem up to now.

The approach presented here differs from other existing approaches in that it uses a generalized mean intensity approach for the solution of the transfer equation. It is the first time that such a generalized mean intensity approach is used in the context of the NLTE radiative transfer problem. At the moment, the code features an advanced solver for the transfer equation, a state of the art solver for the rate equation part, and an iterative coupling between the two. Extended Sobolev theory is used for the treatment of optically thick lines. Its main advantages lie in the transfer part, in its h-independence, the use of a modern, iterative solver, and the modest memory requirements of this part. The code has been successfully tested for some simple NLTE radiative transfer problems and in its present state is on the break of being applied to 'real' problems. So far, we had no possibility to compare our code with other codes.

The problem of multidimensional NLTE radiative transfer is one of the most demanding problems to be solved in numerical astrophysics. The presented approach, which brings together astrophysical knowledge and modern and advanced

numerical techniques, is a contribution to this project. Hopefully the mathematical community will continue to contribute to the solution of this problem.

References

[1] Dykema,P.G. and Klein, R.I. and Castor, J.I. *A new scheme for multidimensional line transfer III. A two-dimensional lagrangian variable tensor method with discontinous finite-element S_n transport,* The Astrophysical Journal, **457** (1996), 892-921.

[2] Fabiani Bendicho, P. and Trujillo Bueno, J. and Auer, L., *Multidimensional radiative transfer with multilevel atoms II. The non-linear multigrid method,* Astronomy and Astrophysics, **324** (1997), 161-176.

[3] Folini, D., *Computational approaches to multidimensional radiative transfer and the physics of radiative colliding flows,* PhD Thesis, Nr. 12606, ETH Zürich, Zürich, (1998).

[4] Hubeny, I., *Accelerated lambda iteration,* in: U.Heber C.S.Jeffery, Eds., The atmospheres of early-type stars, Springer Verlag, (1992), 377-392.

[5] Kanschat, G., *Parallel and adaptive Galerkin methods for radiative transfer problems,* PhD Thesis, Ruprecht-Karls-Universität, Heidelberg, (1996).

[6] Le Bourlot, J. and Pineau des Forêts, G. and Roueff, E., *Complex dynamical behavior in interstellar chemistry,* Astronomy and Astrophysics, **297** (1995), 251-260.

[7] Rybicki, G.B. and Hummer, D.G., *An accelerated lambda iteration method for multilevel radiative transfer I. Non-overlapping lines with background continuum,* Astronomy and Astrophysics, **245** (1991), 171-181.

[8] Stone, J.M. and Mihalas, D. and Norman, M.L. *Zeus-2D: A radiation magnetohydrodynamics code for astrophysical flows in two space dimensions. III. The radiation hydrodynamic algorithms and tests,* The Astrophysical Journal Supplemental Series, **80** (1992), 819-845.

[9] Turek, S., *An efficient solution technique for the radiative transfer equation,* Impact of Computation in Science and Engineering, **5** (1993), 201-214.

[10] Turek, S., *A generalized mean intensity approach for the numerical solution of the radiative transfer equation,* Technischer Report, Interdisziplinäres Zentrum für wissenschaftliches Rechnen, Universität Heidelberg, (1994).

[11] Van der Vorst, H.A., *Bi-CGStab: A fast and smoothly converging variant of Bi-CG for the solution of nonsymmetric linear systems,* SIAM J. Sci. Stat. Comput., **13** (1992), 631-644.

[1]Institut für Astronomie, HAA C15, ETH Zentrum, 8092 Zürich, Switzerland
[2]Seminar für Angewandte Mathematik, ETH Zentrum, 8092 Zürich, Switzerland
[3]Observatoire de Strasbourg, Université Louis Pasteur, Strasbourg, France
E-mail address: folini@astro.phys.ethz.ch,
http://astro.phys.ethz.ch/staff/folini/folini.html